

A biogenerated polymetallic catalyst from society's wastes

Oreste Piccolo^{1*}, Stefano Paganelli², Pietro Zanatta², Sebastiano Tieuli², Laura Sperni², Franco Baldi², Michele Gallo², Iztok Arčon^{3,4}, Katarina Vogel-Mikuš⁵

¹ SCSOP, via Bornò 5, 23896 Sirtori (LC), Italy. Corresponding author e-mail address: orestepiccolo@tin.it;

² Dipartimento di Scienze Molecolari e Nanosistemi, Università Ca' Foscari Venezia, 30172 Venezia Mestre, Italy

³ University of Nova Gorica, Nova Gorica 5000, Slovenia

⁴ Institut Jozef Stefan, Ljubljana 1000, Slovenia

⁵ Department of Biology, Biotechnical Faculty, University of Ljubljana, Ljubljana 1000, Slovenia

ABSTRACT

Aims: Preparation of the new metals-polymeric composite, Met_x-EPS (I), to be used as a green catalyst in water or in two-phase aqueous conditions.

Study design: Recovery and valorization of polymetallic wastes to obtain directly new catalysts using a microorganism to explore their application in removal of difficult and dangerous chemical pollutants present in aqueous environment.

Place and Duration of Study: Dipartimento di Scienze Molecolari e Nanosistemi, Università Ca' Foscari Venezia, Venezia Mestre, Italy; University of Nova Gorica, Nova Gorica, Slovenia, Institut Jozef Stefan, Ljubljana, Slovenia and Department of Biology, Biotechnical Faculty, University of Ljubljana, Ljubljana, Slovenia, between February 2018 and January 2019.

Methodology: For the preparation of Met_x-EPS (I), the metals source was an exhausted catalytic converter that was grinded and treated with an acidic solution at 20-25°C. After filtration, the solution was concentrated, neutralized and added to a broth of *Klebsiella oxytoca* DSM 29614 to produce (I) where metals are embedded in a peculiar polysaccharide structure. The composite was easily recovered from the fermentation broth and purified. The process protocol was verified many times and was shown to be reproducible satisfactorily. The % recovery of metals, originally present in the converter, was good as determined by atomic absorption. The morphology and the chemical state of main metals in (I) were investigated by X-ray absorption spectroscopy methods (XANES and EXAFS). No metallic alloy seems to be evident.

Results: As first application of (I) as catalyst, the hydrodechlorination treatment of polychlorinated biphenyls (PCBs) was studied in water/methanol. A significant removal of higher chlorinated congeners was observed working at 1MPa of hydrogen and 60°C. This result improves significantly and surprisingly the methodology, previously studied by us using mono- or bi-metals embedded in the same polysaccharide moiety, indicating that

positive synergies among the different metals were operating.

Conclusion: The preparation of this new polymetallic species embedded in a polysaccharide moiety starting from spent catalytic converters represents an alternative valorisation of metallic wastes. Moreover, a synergic effect was exerted by the different metals when the catalyst Met_x-EPS (I) was used in the hydrodechlorination treatment of polychlorinated biphenyls (PCBs) in water/methanol. Finally, a promising preliminary proof of concept for the removal of polychlorinated aromatic pollutants even in contaminated aqueous sites was carried out.

Keywords: Metals-polymeric composite; biogenerated polymetallic exopolysaccharide; new catalyst from metallic wastes; hydrodechlorination of PCBs in water

1. INTRODUCTION

As now requested by the circular economy, valuable metals have to be recovered from industrial scraps, such as for example exhausted catalytic converters. Current approaches to treat relevant metallic waste categories are based on pyrometallurgical, hydrometallurgical or bio-hydrometallurgical methods, which present advantages and disadvantages in terms of energy consumption, use of special equipments and difficulty in the purification [1,2]. Then a following treatment is necessary to produce metallic catalysts. To overcome these drawbacks and to obtain directly a composite useful as catalyst, our protocol at first treats grinded exhausted catalytic converters at room temperature with a concentrated acidic solution, such as aqua regia or 80% nitric acid, to dissolve metals as ions and, after filtration of the solid residue, concentration and neutralization of the solution, takes advantage of the property of a plurimetal resistant microorganism *Klebsiella oxytoca* DSM 29614. This microorganism is able to generate, in the presence of heavy metal cations, a specific capsular exopolysaccharide (EPS) which may embed them and then be extruded from the cell so to be easily purifiable [3-4]. So a new metals-polymeric composite, Met_x-EPS (I) was obtained from exhausted catalytic converters and, after characterization with different methods, its catalytic activity and a possible synergic effect due to the presence of different metals embedded in EPS was verified in the hydrodechlorination treatment of a methanolic solution of polychlorinated biphenyls (PCBs) in distilled water and in a sample of polluted sea water (Mar Piccolo, Taranto, Italy). The results were compared with those recently obtained by us using Pd-EPS or Pd,Fe-EPS [5].

2. MATERIAL AND METHODS / EXPERIMENTAL DETAILS / METHODOLOGY

2.1 Materials and Instrumentation

Nutrient broth (Difco), n-hexane (pesticide grade; Romil), PCB standards (AccuStandard) were utilised. Aroclor 1260 and the other reagents were Sigma-Aldrich products and used as received. The total amounts of elements were determined versus their relative standards solutions by inductively coupled plasma atomic emission spectrometry (ICP-AES) (Optima 3100, Perkin Elmer). The FT-IR spectra (KBr pellets) of Met_x-EPS were recorded on an FT-IR Nicolet Magna 750 instrument. X-ray absorption spectra were measured on of Met_x-EPS sample in the energy range of K or L3 absorption edges of constituent metal cations (Pd K-edge (24350 eV), Rh K-edge (23220 eV), Zr K-edge (17998 eV), Pt L3 edge (11564 eV), Ce L3 edge (5724 eV)) to obtain corresponding XANES (X-ray Absorption Near Edge Structure) and EXAFS (Extended X-ray Absorption Fine Structure) spectra of the investigated elements. The Met_x-EPS sample was prepared in the form of homogeneous self-standing pellets, each optimised to provide the total absorption thickness (μd) of about 1.5 above the investigated absorption edges. All absorption spectra were measured at room temperature in transmission detection mode at two different synchrotron radiation facilities (Zr, Pt and Ce at

68 XAFS beamline at Elettra in Trieste, Italy; Pd and Rh at BL22 (Claess) beamline of ALBA in
69 Barcelona, Spain); a Si (111) double crystal monochromator was used at the XAFS
70 beamline of the Elettra and a Si(311) at BL22 of ALBA. The intensity of the monochromatic
71 X-ray beam was measured by three consecutive ionization detectors. The samples were
72 placed between the first pair of detectors. The exact energy calibration was established with
73 simultaneous absorption measurement on the corresponding reference metal foil placed
74 between the last pair of detectors. Absolute energy reproducibility of the measured spectra
75 was ± 0.03 eV. The absorption spectra were measured within the interval [-150 eV to 1000
76 eV] relative to the investigated absorption edge. In the XANES region, equidistant energy
77 steps of 0.5 eV were used, while for the EXAFS region, equidistant k-steps ($\Delta k = 0.03 \text{ \AA}^{-1}$)
78 were adopted, with an integration time of 1 s per step. The quantitative analysis of XANES
79 and EXAFS spectra is performed with the IFEFFIT program package [6] in combination with
80 FEFF6 program code [7] for ab initio calculation of photoelectron scattering paths. The
81 determination of PCB congeners was performed in full scan mode on a fused silica capillary
82 column (HP5-MS 30 m, 0.25 mm x 0.25 mm; Agilent Technologies) installed in a
83 ThermoFinnigan (Trace GC 2000) coupled to a quadrupole mass spectrometer
84 (ThermoFinnigan Trace MS), using the same conditions described in our previous work [5].
85

86 **2.2 Recovery of acidic metallic solutions from grinded exhausted catalytic 87 converters and preparation of a new metals-polymeric composite (I)**

88 As typical procedure, grinding and pulverizing 20 g of exhausted catalytic converter was
89 carried out using a mortar. The obtained powder was transferred to a 1 liter flask, into which
90 400 mL of 80% HNO_3 or of aqua regia [65% HNO_3 : 37% HCl (1:3)] was poured under
91 stirring; after 24 h at 20-25°C the mixture was filtered and the residue solid washed with
92 distilled water; the filtrate was then concentrated at reduced pressure up a volume of 80 mL.
93 This solution was split in two parts, one was used for quantitative analyses of the extracted
94 metals (**Table A**), the other (40 mL) was neutralized to pH 7.0 with a concentrated NaOH
95 solution until a final volume of 50 mL and immediately added to a culture of *Klebsiella*
96 *oxytoca*, DSM 29614 in 1 liter of NaC medium, which contained minimum minerals and
97 sodium citrate as sole carbon and energy source, and had been prepared adapting the
98 protocol already described in our previous works [3, 4]. The culture was grown under
99 anaerobic conditions for 5 days and when a cell density upper than 1.0 Abs at 600 nm was
100 reached, 50 ml of instantly buffered plurimetallic sample were added. After 48 h from this
101 addition, the cell culture was put in a centrifuge to eliminate bacterial cells. The supernatant
102 was treated with 800 ml of cooled 95% ethanol to precipitate Met_x -EPS. The purification
103 procedure was repeated twice. After drying under vacuum, the material was finally grinded to
104 powder to obtain 1-1.3g of polymetallic polysaccharide. The preparation of (I) using metals
105 recovered by aqua regia treatment was repeated for three times verifying good
106 reproducibility of the results.
107

108 **2.3 Element determination in a new metals-polymeric composite (I)**

109 Samples (1 mg) of dry pulverized polymetallic composites were digested with 2 ml of aqua
110 regia, heating the mixture at 60°C until a complete dissolution for element determination.
111 The recovery yield of the main metals is reported in **Table A**.
112

113 **2.4 Optimized protocol of hydrodechlorination of Aroclor 1260 using the new 114 catalyst (I)**

115 A suitable amount of Met_x -EPS (I) to obtain a substrate/Pd $\approx 8/1$ mol ratio (8.8 mg) was
116 stirred in a Schlenk tube under nitrogen in 4 ml of distilled water or 4 ml of Mar Piccolo
117 (Taranto, Italy) water for about 10 min. A solution of 7 mg of Aroclor 1260 (~ 0.0195 mmol
118 assuming MW 358 as medium value) in 2 ml of methanol was then added to the aqueous
119 phase as well as 1.7 mg (0.021 mmol) of ammonium acetate. The Schlenk tube was then
120 transferred into a 150 ml stainless steel autoclave under nitrogen, pressurized with 1 MPa of

121 H₂, instead of 3MPa used previously with Pd-EPS or Pd,Fe-EPS [5], and stirred at 60°C for
 122 20 h. The reactor was then cooled to room temperature and opened under nitrogen. Then,
 123 the organic products were separated from the catalyst extracting them from the aqueous
 124 phase with 10 mL of n-hexane. The procedure of extraction was repeated three times. The
 125 organic phases were collected and dried on Na₂SO₄, then concentrated using a nitrogen flow
 126 (Turbovap 2, Caliper Science) and analyzed by GC-MS.

127
 128

129 3. RESULTS AND DISCUSSION

130
 131

132

133 3.1 Catalyst characterization

134 The results of elemental determination are reported in **Table A**.

135

136 **Table A.** Main metals extracted from exhausted catalytic converters and present in Met_x-
 137 EPS^a.

Analyzed Metals	C (mg/L) HNO ₃ (n.a.) sol. (inc. ±10%)	C (mg/L) aqua regia (a.r.) sol. (inc. ±10%)	(Met _x EPS) _{n.a.} Metal recovery yield% ^b	(Met _x EPS) _{a.r.} Metal recovery yield% ^b
Pd	428	748	89	99
Pt	31.9	479	81	83
Rh	2.07	111	84	85
Al	1623	2413	80	>99
Ce	nd	2158	nd	99
Zr	nd	nd	nd	nd
W	121	174	29	10

138 ^a Experimental conditions: 20 g of exhausted catalytic converter; 400 ml of 80% HNO₃ or
 139 acqua regia; T = 20°C; t = 24 h; final volume of the acidic solution after distillation = 80 ml. ^b
 140 (Amount of metal encapsulated in EPS)/(amount of metal present in the starting acidic
 141 solution)%. nd = not determined

142

143 Even if the aqua regia treatment is, as expected, more efficient to extract metals from
 144 exhausted catalytic converters, the % of recovery of metals, bonded or encapsulated in the
 145 new composite, after the biological treatment, is not significantly affected and is very high
 146 (80->99%) with the exception of tungsten (**Table A**).

147 As already described in more detail [8], Met_x-EPS (I) was characterized by FT-IR and by the
 148 x-ray absorption spectroscopy methods XANES and EXAFS. The IR spectrum (**Appendix**,
 149 **Fig. 1**) confirmed the presence of metals bound to capsular EPS. It looks quite similar to the
 150 spectrum of a previous prepared Pd-EPS [4] but with a very intense sharp band at 1384
 151 cm⁻¹. The intense symmetric stretching of COO⁻ vibration to 1384 cm⁻¹, on the basis of
 152 literature, should demonstrate, in our opinion, that carboxyl group was a contributor in the
 153 sorption of metals [9, 10]. In the region between 1550-1650 cm⁻¹ it is possible to observe
 154 two peaks, one of them or both could be due to the asymmetric stretching of COO⁻ vibration
 155 bounded to metals [9]. Indeed the EPS is formed by an eptameric structure with two D-

156 glucuronic acids, four L-rhamnose, and one D-galactose [11]. However it is not possible to
157 exclude also contribution of nitrogen species such as any nitrogen heterocyclic compounds
158 eventually formed during the fermentation or membrane protein amide bonds [9]. Finally,
159 the other intense peak at 1065 cm^{-1} , as it was already observed for other similar metal EPS,
160 is to attribute to phosphate groups [4, 10].

161 The presence of metals bounded to capsular EPS and valence and structural information of
162 metal cations in the $\text{Met}_x\text{-EPS}$ complex at the atomic scale were confirmed by x-ray
163 absorption spectroscopy methods XANES and EXAFS [8]. It is known that, in the XANES
164 spectrum, an increase of oxidation state results in a shift of each absorption feature to higher
165 energies [4, 12]. The Pd K-edge profile of the Pd in the $\text{Met}_x\text{-EPS}$ complex are identical to
166 the Pd XANES spectrum of the Pd metal foil with fcc crystalline structure and also to FePd-
167 EPS(A), FePd-EPS(B) and Pd-EPS samples, previously reported by us [4]. It clearly
168 indicates that palladium also in (I) is predominantly as Pd (0) (Appendix, Fig. 2a).

169 Results of Pd K-edge EXAFS analysis (Appendix, Fig. 2b) suggested that Pd in (I) is in the
170 form of Pd(0) metallic nano-particles with fcc crystalline structure, similar to that found in
171 mono- and bi-metallic (Pd-EPS and FePd-EPS) samples from previous investigations [4].
172 However smaller nano-clusters of Pd metal are formed and the average size of Pd metal
173 nanoparticles is less than 1 nm (Appendix, Table 1). Furthermore, in EXAFS analysis of Pd
174 neighborhood, we found that part of Pd atoms is coordinated to oxygen atoms at about 1.97
175 Å which is characteristic for Pd oxides (Appendix, Table 1). So it is possible that about 10%
176 of Pd atoms is in the form of PdOx nanoparticles simply encapsulated in the polysaccharide
177 moiety or that Pd atoms located on the surface of the Pd metallic nanoparticles may be
178 bonded to the OH or COOH groups of EPS. The results (Appendix, Fig. 2b) are similar, but
179 not identical, to those observed on mono- and bi-metallic samples [4].

180 The Pt L3-edge XANES analysis would suggest that there are two forms of Pt in (I), one is
181 metallic Pt(0) nanoparticles (about 36 %), as expected, the other in the form of a Pt(II)
182 complex bound to two Cl atoms and two nitrogen atoms like in $\text{PtCl}_2(\text{pyridine})_2$ (Appendix,
183 Fig 3a) [13]. Pt L3-edge EXAFS results strongly support this finding (Appendix, Fig 3b,
184 Table 2). The results clearly suggest that microorganism *Klebsiella oxytoca* encapsulates Pt
185 species in EPS partly in the form of metallic Pt(0) nanoparticles and partly in the form of
186 complexes structurally similar to $\text{PtCl}_2(\text{pyridine})_2$. It is difficult to have a clear-cut explanation
187 for the latter form. Maybe PtCl_2 , originally added to the fermentation broth, can bind to
188 nitrogen heterocyclic species, e.g. piperazine derivatives, probably formed during the
189 fermentation process [14].

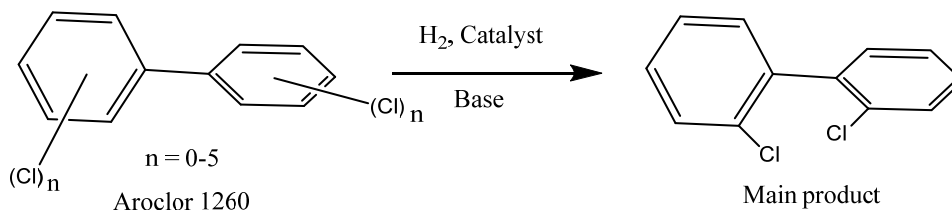
190 The Ce L3-edge XANES analysis (Appendix, Fig. 4) and the comparison with CeVO_4 and
191 CeO_2 XANES spectra showed that all Ce in the $\text{Met}_x\text{-EPS}$ sample is in the form of three
192 valent Ce cations, most probably in the form of Ce^{3+} oxide nanoparticles [15]. Finally the
193 results of Zr and Rh EXAFS analysis of $\text{Met}_x\text{-EPS}$ sample (Appendix, Figs. 5 and 6)
194 suggested that both elements, Zr and Rh, are in oxidized form, as a mixture of different Zr
195 and Rh nano-oxides. Zr-Zr distances are characteristic for Zr oxides [16] while Rh-Rh
196 distances are characteristic for crystalline Rh_2O_3 [17]. Also Ce, Zr or Rh cations
197 coordination to OH and COOH groups cannot be excluded.

198
199
200

201 3.2 Catalyst activity

202 Removal of polychlorinated pollutants present in water by catalysed hydrodechlorination is
203 still a challenging target due to the presence of different catalyst poisons. As part of our
204 research activity in environmental remediation and in finding potential sustainable protocols
205 using heterogeneous water compatible catalysts we had recently studied the
206 hydrodechlorination of a methanolic solution of Aroclor 1260 (a reference PCB mixture) with
207 Pd-EPS and Fe,Pd-EPS in pure distilled water in the presence of ammonium acetate [5]
208 (Scheme 1).

209
210

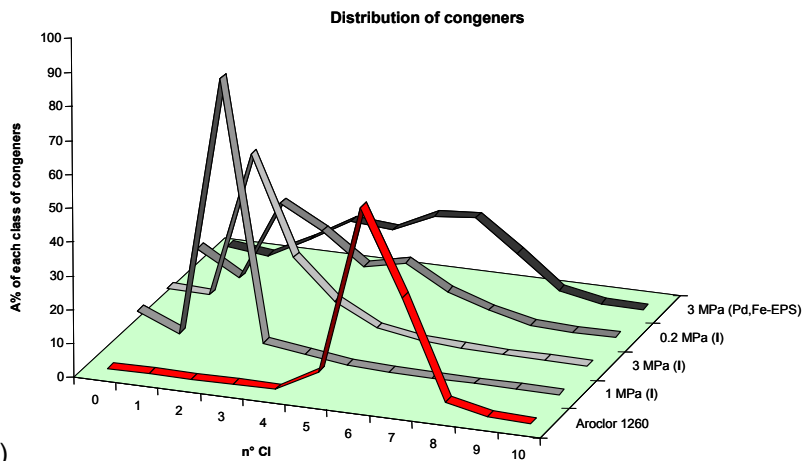


211
212
213
214

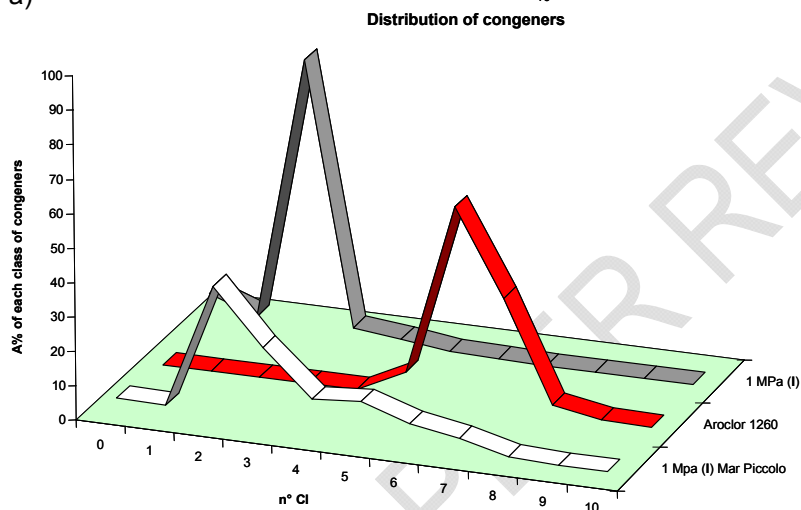
Scheme 1. Hydrodechlorination of Aroclor 1260.

215
216
217
218
219
220
221
222
223
224
225
226
227
228

An improvement in the dehalogenation reaction using the bimetallic catalyst had been observed working at a pressure of 3MPa of hydrogen with a substrate/catalyst 8/1 molar ratio (referred to Pd amount), at 60°C in 20 h, but a relevant amount of Cl₅-Cl₇ congeners was still present. Therefore we were encouraged to test this new polymetallic (Met_x-EPS) (I) on the same substrate to try to improve our previous results, working either in pure distilled water or diluting this PCBs mixture in a sample of polluted sea water taken from Mar Piccolo (Taranto, Italy) which contained also other pollutants such as PAHs and heavy metals. Quite surprising, very stimulating and promising results were achieved working under much milder reaction conditions. As shown in Fig. 1a it was possible to obtain a complete removal of congeners having a content of chlorine atoms >3 working at a pressure of 1MPa of hydrogen with the same substrate/catalyst 8/1 molar ratio (referred to Pd amount). Quite satisfactory results were also obtained using a real polluted water spiked with Aroclor 1260 as depicted in Fig. 1b.



229 a)



230

231

232

233

234

235

236

237

238

239

240

241

242

243

244

245

246

247

248

249

250

b)

Fig. 1. Hydrodechlorination of Aroclor 1260 results compared with previous best results [5]: a) in pure water; b) diluting Aroclor 1260 in polluted sea water of Mar Piccolo

It indicates that this new catalyst is quite robust and is able of working in water and of resisting to the poisoning. Synergic positive effects due to the presence of polymetals were clearly demonstrated either in the hydrodechlorination reaction or in the ability to break down/reduce the amounts of palladium poisons present in the polluted sea water. Furthermore PCBs concentrations of some very toxic dioxin-like PCBs congeners: BZ 118, 156, 157, 167, 170, 180, 189 in Aroclor 1260 were reduced to nearly zero (A%) (Table B) using this new catalyst and it is a significant improvement in the used protocol.

251 **Table B.** PCBs concentrations of some dioxin-like PCBs congeners: BZ 118, 156, 157, 167,
252 170, 180, 189 in Aroclor 1260 and in the product obtained after hydrogenation in the
253 presence of Pd, Fe-EPS or Met_x-EPS(I)
254

BZ Number of some dangerous PCBs congeners ^a	Aroclor 1260 A %	Pd,Fe-EPS A % (3 MPa of H ₂) ^b	Met _x -EPS(I) A % (1 MPa of H ₂)
118 (+149)	10.18	5.16	0.04
156 (+173)	1.84	0.39	nd
157 (+197)	0.31	0.07	nd
167	0.72	0.29	nd
170 (+190)	4.25	1.33	nd
180	8.88	3.27	nd
189	0.13	0.02	nd

255 ^a congeners number according to Ballschmiter K, Zell M(1980) Analysis of Polychlorinated
256 Biphenyls (PCB) by Glass Capillary Gas Chromatography. Fresenius Z Anal Chem 302: 20-
257 31; ^b see ref. [5]; nd = not detected
258

259
260
261
262

263 4. CONCLUSION

264
265
266
267
268
269
270
271
272
273
274
275
276
277

The present work shows that our idea of preparing a new polymetallic catalyst from spent catalytic converters, combining a chemical treatment and the following action of a plurimetal resistant microorganism *Klebsiella oxytoca* DSM 29614, was realized efficiently.

Positive synergies among the different metals, embedded in a peculiar polysaccharide moiety, were found when Met_x-EPS (I) was used as a catalyst in the removal of PCBs by hydrodechlorination reaction, permitting to work under milder conditions with a better efficacy than our previous studies where mono- or bimetallic Pd species prepared by the same microorganism had been used [5]. This result was not easily predictable, especially when the reaction was carried out in the presence of a sample of real water taken from a contaminated site.

So this catalyst seems quite robust and potentially useful to be applied for the remediation of water taken from polluted areas.

278
279

280 COMPETING INTERESTS

281
282

The authors declare no conflict of interest.

283
284

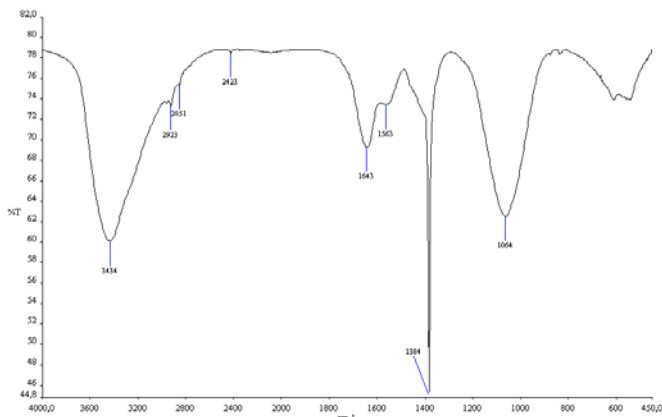
285 REFERENCES

286
287
288
289
290
291
292

- [1] Jadhav UU, Hocheng H, Achiev J. A review of recovery of metals from industrial waste. *Mat. Manufacturer Eng.* 2012; 54: 159-167.
- [2] Izatt RM, Izatt SR, Bruening RL, Izatt NE, Moyer BA. Challenges to achievement of metal sustainability in our high-tech society. *Chem. Soc. Rev.* 2014; 43: 2451-2475.
- [3] Baldi F, Marchetto D, Paganelli S, Piccolo O. Bio-generated metal binding polysaccharides as catalysts for synthetic applications and organic pollutant transformations. *New Biotechnology* 2011; 29: 74-78.

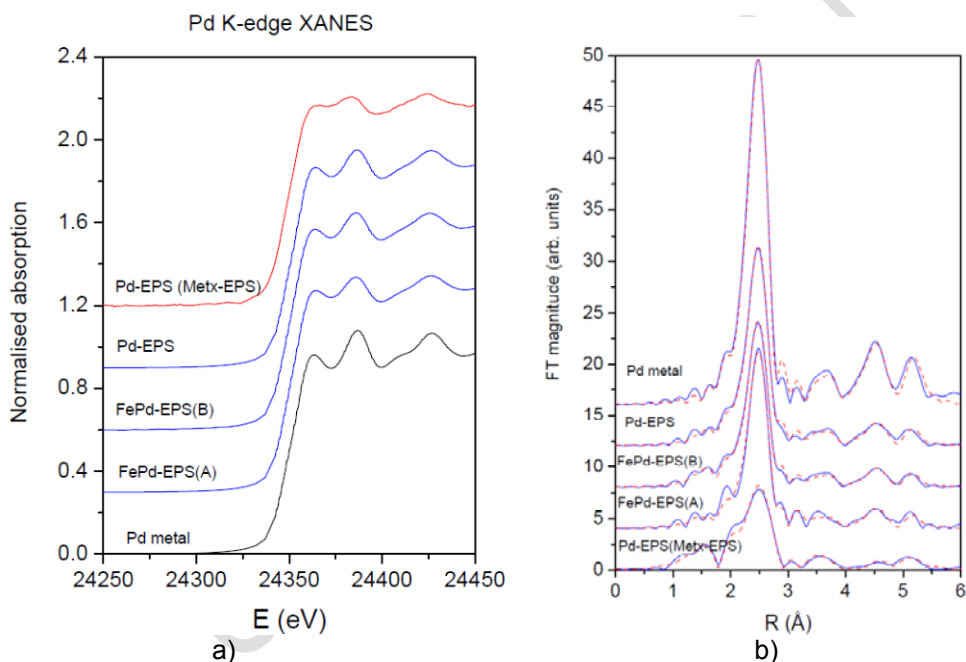
- 293 [4] Arčon I, Paganelli S, Piccolo O, Gallo M, Vogel-Mikuš K, Baldi F. XAS analysis of iron
294 and palladium bonded to a polysaccharide produced anaerobically by a strain of *Klebsiella*
295 *oxytoca*. J. Synchrotron Rad. 2015; 22: 1215-1226.
- 296 [5] Baldi F, Gallo M, Paganelli S, Tassini R, Sperti L, Piccolo O, et al. Hydrodechlorination
297 of Aroclor 1260 in Aqueous Two-phase Mixture Catalyzed by Biogenerated Bimetallic
298 Catalysts. Int. Res. J. Pure & Appl.Chem. 2016; 11: 1-9 and loc. ref.
- 299 [6] Ravel B, Newville M. **ATHENA, ARTEMIS, HEPHAESTUS**: data analysis for X-ray
300 absorption spectroscopy using **IFEFFIT**. J. Synchrotron Rad. 2005;12: 537-541.
- 301 [7] Rehr JJ, Albers RC, Zabinsky SI. High-order multiple-scattering calculations of x-ray-
302 absorption fine structure. Phys. Rev. Lett. 1992; 69: 3397-3400.
- 303 [8] Tieuli S, Baldi F, Arčon I, Vogel-Mikuš K, Gallo M, Sperti L, et al.. **Alternative Recovery**
304 **and Valorization of Metals from Exhausted Catalytic Converters in a New Smart Polymetallic**
305 **Catalyst. ChemistrySelect, 2019; 4 : (in press)**
- 306 [9] Papageorgiou SK, Kouvelos EP, Favvas EP, Sapalidis AA, Romanos GE, Katsaros FK.
307 Metal-carboxylate interactions in metal-alginate complexes studied with FTIR spectroscopy.
308 Carbohydr. Res. 2010; 345: 469-473.
- 309 [10] Tan L, Dong H, Liu X, He J, Xu H , Xie J. Mechanism of palladium(II) biosorption by
310 *Providencia vermicola*. RSC Adv. 2017; 7: 7060-7072.
- 311 [11] Leone S, De Castro C, Parrilli M, Baldi F, Lanzetta R. Structure of the Iron-Binding
312 Exopolysaccharide Produced Anaerobically by the Gram-Negative Bacterium *Klebsiella*
313 *oxytoca* BAS-10. Eur.J.Org. Chem 2007; 5183-5189.
- 314 [12] Wong J, Lytle FW, Messmer RP, Maylotte DH. K-edge absorption spectra of selected
315 vanadium compounds. Phys. Rev. B 1984; 30: 5596-5610.
- 316 [13] Arčon I, Kodre A, Abra RM, Huang A, Vallne JJ, Lasič DD, Colloids and Surfaces B:
317 Biointerfaces , 2004, 33, 199-204.
- 318 [14] Meng W, Xiao D, Wang R. Enhanced production of tetramethylpyrazine in *Bacillus*
319 *licheniformis* BL1 by *bdhA* disruption and 2,3-butanediol supplementation. World J.
320 Microbiol. Biotechnol. 2016; 32: 32-46.
- 321 [15] Kozjek Škofic I, Padežnik Gomilšek J, Kodre A, Bukovec N, Solar Energy Materials &
322 Solar Cells , 2010, 94 , 554-559.
- 323 [16] Bouvier P, Djurado E, Ritter C, Dianoux AJ, Lucazeau G. Low temperature phase
324 transformation of nanocrystalline tetragonal ZrO₂ by neutron and Raman scattering studies.
325 Int. J. Inorg. Mater. 2001; 3: 647-654.
- 326 [17] Coey JMD. The crystal structure of Rh₂O₃. Acta Cryst. 1970; B 26: 1876-1877.
- 327

328 APPENDIX
329
330



331
332
333 **Fig. 1.** FT-IR spectrum of Met_x-EPS
334

335



336
337
338
339
340
341
342
343
344
345

Fig. 2. a) Pd K-edge XANES spectra of the Pd-species in Met_x-EPS sample compared to Pd-EPS, FePd-EPS(A), FePd-EPS(B) samples and reference Pd metal foil with f.c.c. crystal structure; b) Pd EXAFS Fourier transform magnitude of k₃-weighted Pd EXAFS spectra of Pd-EPS, FePd-EPS(A), FePd-EPS(B), Pd-species in Met_x-EPS samples and Pd metal foil, calculated in the k range 3–16 Å⁻¹ and R range 1–5.5 Å. Experiment: solid line; best-fit EXAFS model of the nearest coordination shells: dashed line.

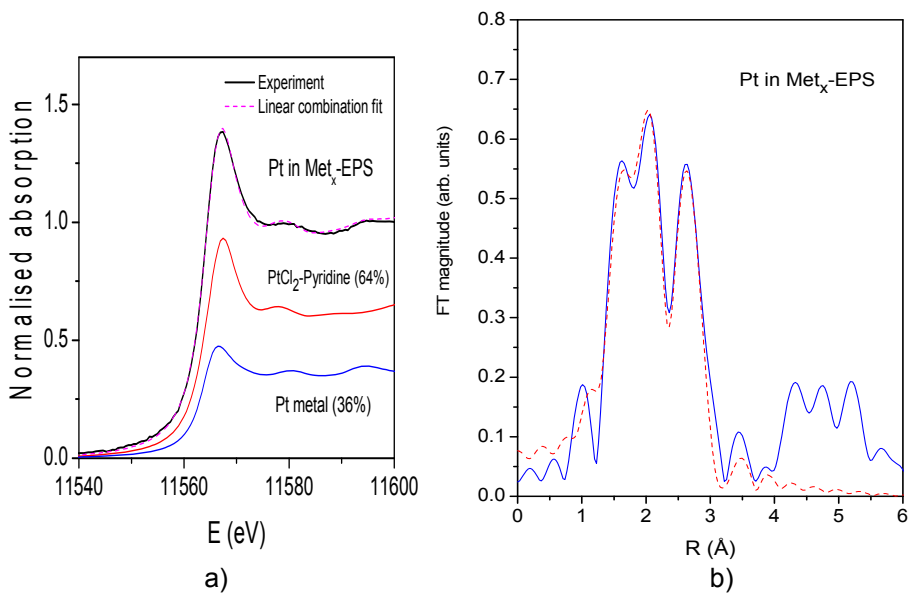


Fig. 3. a) Pt L3-edge XANES spectrum measured on the Pt in Met_x-EPS sample: Black solid line: experiment; magenta dashed line: best-fit linear combination of XANES profiles of Pt fcc metal (36%), and cis-dichlorobis pyridine platinum reference compound (64%); b) Fourier transform magnitude of k²-weighted Pt L3-edge EXAFS spectra of Pt in Met_x-EPS sample, calculated in the k range 3–12 Å⁻¹ and R range 1–3.8 Å. Experiment: solid line; best-fit EXAFS model of the nearest coordination shells: dashed line.

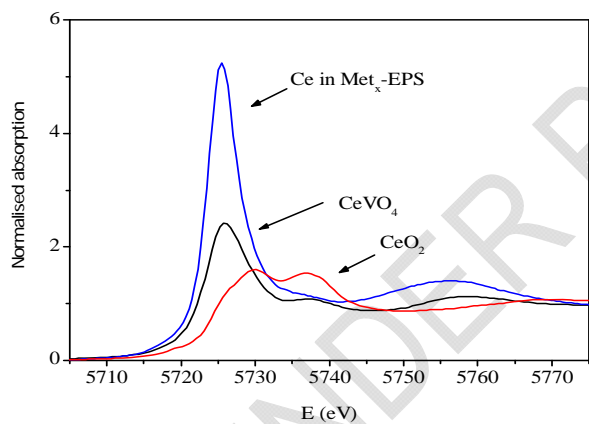
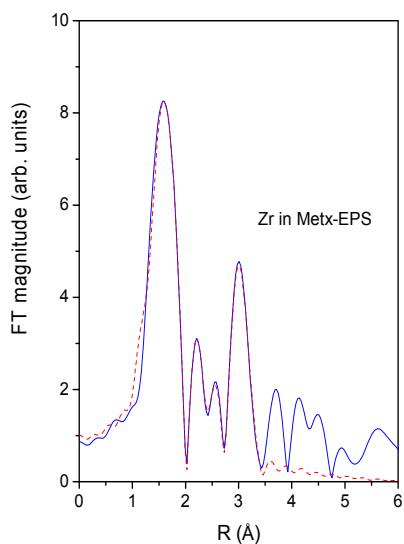
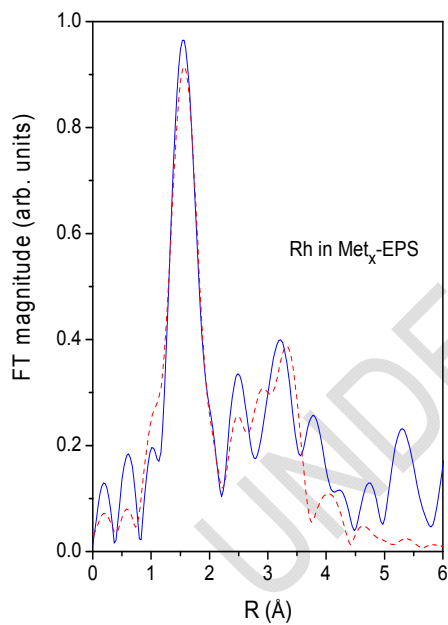


Fig. 4. Ce L3-edge XANES spectra of the Ce species in Met_x-EPS sample compared to CeVO₄ and CeO₂ spectra as references for Ce³⁺ and Ce⁴⁺, respectively.



365
 366 **Fig. 5.** Fourier transform magnitude of k_3 -weighted Zr K-edge EXAFS spectra of Zr in Met_x -EPS sample, calculated in the
 367 k range $3\text{--}11 \text{ \AA}^{-1}$ and R range $1\text{--}3.4 \text{ \AA}$. Experiment: solid line; best-fit EXAFS model of the nearest coordination shells:
 368 dashed line.
 369
 370



371
 372
 373
 374
 375
 376 **Fig. 6.** Fourier transform magnitude of k_2 -weighted Rh K-edge EXAFS spectra of Rh in Met_x -EPS sample, calculated in
 377 the k range $3\text{--}11 \text{ \AA}^{-1}$ and R range $1\text{--}3.4 \text{ \AA}$. Experiment: solid line; best-fit EXAFS model of the nearest coordination shells:
 378 dashed line.
 379
 380
 381
 382

Table 1. Parameters of the nearest coordination shells around Pd atoms in Met_x-EPS sample and in reference Pd metal foil with fcc crystal structure (a=3.8900 Å): average number of neighbour atoms (*N*), distance (*R*), and Debye-Waller factor (σ^2). Uncertainty of the last digit is given in parentheses. A best fit is obtained with the amplitude reduction factor $S_0^2 = 0.87$. The goodness-of-fit parameter, *R*-factor, is given in the last column.

Pd neigh.	<i>N</i>	<i>R</i> [Å]	σ^2 [Å ²]	<i>R</i> -factor
Pd in the Met _x -EPS sample				
O	1.4(2)	1.97(1)	0.005(2)	
Pd	0.6(3)	3.50(4)	0.008(4)	
Pd	5.3(6)	2.749(4)	0.0075(6)	0.014
Pd	4(2)	3.91(1)	0.013(1)	
Pd	7(2)	4.77(1)	0.013(1)	
Pd	7(3)	5.53(1)	0.013(1)	
Reference Pd metal foil				
Pd	12	2.745(2)	0.0058(2)	0.003
Pd	6	3.896(2)	0.0086(5)	
Pd	24	4.772(2)	0.0088(5)	
Pd	12	5.510(2)	0.0090(5)	

Table 2. Parameters of the nearest coordination shells around Pt atoms in Met_x-EPS sample: average number of neighbour atoms (*N*), distance (*R*), and Debye-Waller factor (σ^2). Uncertainty of the last digit is given in parentheses. A best fit is obtained with the amplitude reduction factor $S_0^2 = 0.91$. The goodness-of-fit parameter, *R*-factor, is given in the last column.

Pt neigh.	<i>N</i>	<i>R</i> [Å]	σ^2 [Å ²]	<i>R</i> -factor
N	1.2(3)	2.04(3)	0.002(1)	0.02
Cl	1.2(3)	2.37(4)	0.003(4)	
Pt	7(3)	2.71(1)	0.013(1)	
C	4.6(8)	2.97(7)	0.003(2)	